*Progress In Electromagnetics Research Letters, Vol. 79, 1–7, 2018*

# A Cavity-Backed Wideband Circularly Polarized Crossed Bowtie Dipole Antenna with Sequentially Rotated Parasitic Elements

**Yapeng Li*, Zhipeng Zhao, Jinhai Liu, and Yingzeng Yin**

**Abstract**—A cavity-backed crossed bowtie dipole antenna for wideband circularly polarization (CP) is proposed in this letter. By introducing four inverted L-shaped parasitic elements with sequentially rotated angles, two extra CP modes are excited, thus greatly broadening the 3-dB Axial-ratio (AR) bandwidth (BW) of the antenna. The proposed antenna is simulated, fabricated and measured. Results show that the antenna generates a 10-dB impedance bandwidth (IBW) of 91.4% (1.2–3.22 GHz) and a 3-dB AR bandwidth of 74.1% (1.37–2.95 GHz). In addition, the antenna achieves a unidirectional radiation pattern with a stable gain of 6.52–9.27 dBi over the whole CP operating band.

## 1. INTRODUCTION

Circularly polarized antennas have been widely used in various wireless communication systems due to their capabilities of reducing faraday rotation effect, suppressing multi-path interference, and reducing polarization mismatch. To generate circular polarization, crossed dipoles fed by two sources with equal magnitude and 90° phase difference are popular candidates [1–4]. Nowadays wide ARBW can be achieved by introducing bowtie-shaped crossed dipoles [5, 6], parasitic elements [7–9] or slots [10, 11]. Due to the Inhomogeneous distribution of currents, only a few of them can generate an overlap bandwidth of more than 50% and maintain radiation patterns and gains stable in the whole operating band at the same time. For example, a printed unidirectional CP antenna with quad-folded dipoles is proposed in [2]. Although the antenna observes stable radiation patterns and gains at the operating band, and the 3-dB ARBW is optimized to only 35%. In [9], a broadband cavity-backed crossed dipole encircled by an asymmetrical cross loop is presented, and the 3-dB ARBW is 53.4%. However, the impedance band and AR band are not well matched.

To solve the problems above, a cavity-backed crossed bowtie dipole antenna is presented in this letter. By employing sequentially rotated parasitic elements, the ARBW is broadened greatly. The simulated and measured results are in good agreement.

## 2. ANTENNA DESIGN AND ANALYSIS

Figure 1 depicts the geometry of the proposed crossed bowtie dipole antenna. The antenna consists of two crossed bowtie dipoles, four inverted L-shaped parasitic elements, and a metal reflector with back cavity. The dipoles and parasitic elements are printed on an F4B substrate ($\varepsilon_r = 2.65$, $\tan\delta = 0.02$, the thickness is 0.035 mm) with a dimension of $90 \times 90 \times 0.8\,\text{mm}^3$. The two pairs of crossed bowtie dipoles are connected by two phase delay lines which provide 90° phase difference. The two lines are separately connected to the inner and outer face of an 50-Ω coaxial line. The four inverted L-shaped parasitic elements have sequentially rotated angles of 45°, 135°, 225° and 315° separately. The main

*Received 8 August 2018, Accepted 7 September 2018, Scheduled 19 September 2018*
* Corresponding author: Yapeng Li (liyapengedu@163.com).
The authors are with the National Key Lab of Antenna and Microwave Technology, Xidian University, Xi'an, Shaanxi 710071, China.

parameters of the proposed antenna are $R_1 = 2.5$, $R_2 = 30$, $R_3 = 4.7$, $R_4 = 40$, $W_1 = 0.8$, $W_2 = 1$ (unit: mm). The height of the coaxial cable and the back cavity are both 40 mm and the metal reflector is $140 \times 140\,\text{mm}^2$.

To elaborate the operation mechanism of the proposed antenna, an evolution process is shown in Figure 2. Three antennas are defined as Ant.1: crossed bowtie dipole with only a back cavity, Ant.2: four bowtie-shaped parasitic elements added, Ant.3: four inverted L-shaped parasitic elements added. The reflection coefficient and AR of the three antennas are shown in Figure 3 for contrast. It can be seen from Figure 3 that Ant.1 has a wide impedance bandwidth with $|S_{11}| < -10\,\text{dB}$ of 80.8% (1.29–3.04 GHz). Although the 3-dB ARBW is only 45.5% (1.53–2.43 GHz), it is obvious that Ant.1 generates two CP resonant modes. When bowtie-shaped parasitic elements are introduced in Ant.2, another CP resonant mode is generated at 2.45 GHz, and AR performance gets better at high frequencies. The ARBW is extended to 63% (1.52–2.92 GHz). Besides, the impedance is broadened slightly at high frequencies. To achieve a broader ARBW, four inverted L-shaped parasitic elements with sequentially rotated angles are introduced in Ant.3, and another CP resonant mode is generated at 1.48 GHz. As a consequence, a wide ARBW of 74.1% (1.35–2.94 GHz) is achieved, and the impedance bandwidth is broadened to 89.9% (1.2–3.16 GHz). The current distribution of the proposed antenna at 1.5 GHz is shown in Figure 4 as an example. It can be seen that the dominant currents flow along the edges of the parasitic elements at each quarter of a period of time, and the synthetic current changes with right hand principle, thus a Right Hand Circular Polarization (RHCP) is generated.

To get a deep insight into the proposed antenna, a parameter study is carried out on radius and rotation angle of the inverted L-shaped parasitic elements.

Figure 5 presents $|S_{11}|$ and AR for different radii of the inverted L-shaped parasitic elements. It can

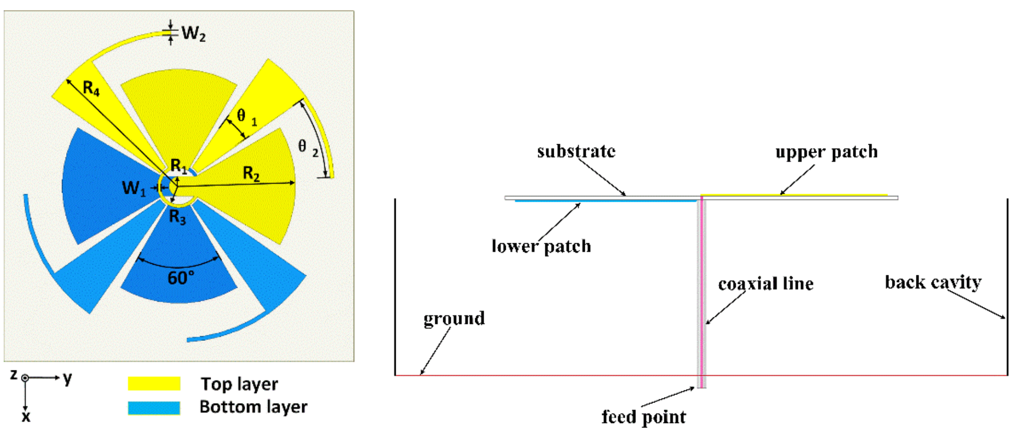


(a) (b)

**Figure 1.** Geometry of the proposed antenna. (a) Top view, (b) side view.

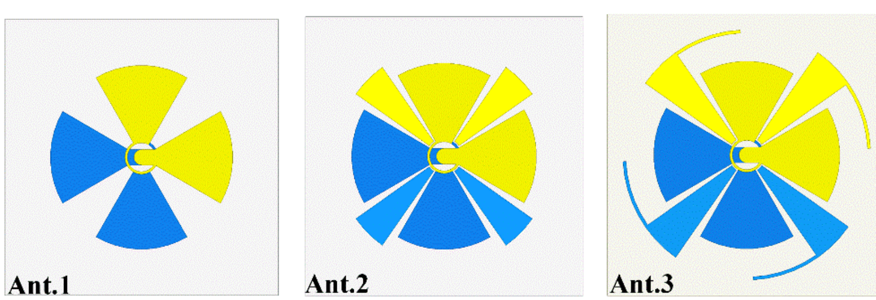


**Figure 2.** Evolution of the antenna.

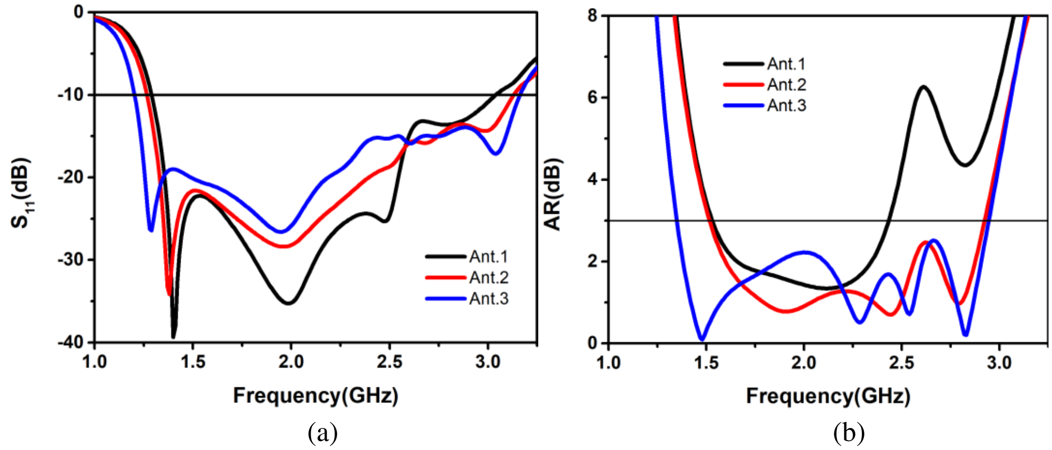


**Figure 3.** Performance of the three antennas. (a) $|S_{11}|$, (b) AR.

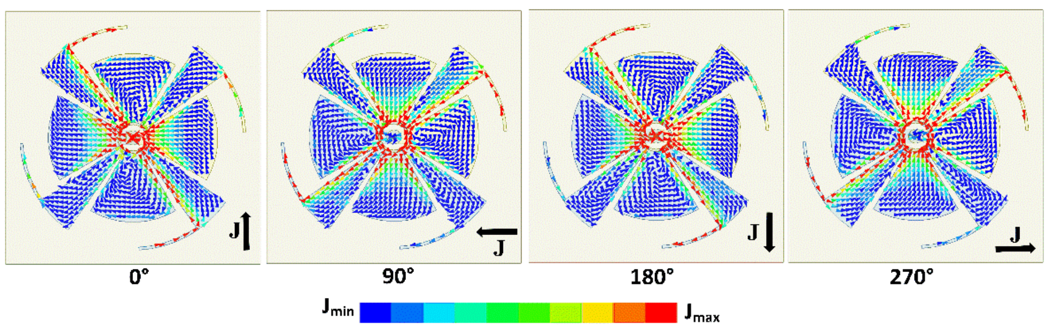


**Figure 4.** Current distribution of the proposed antenna at 1.5 GHz.

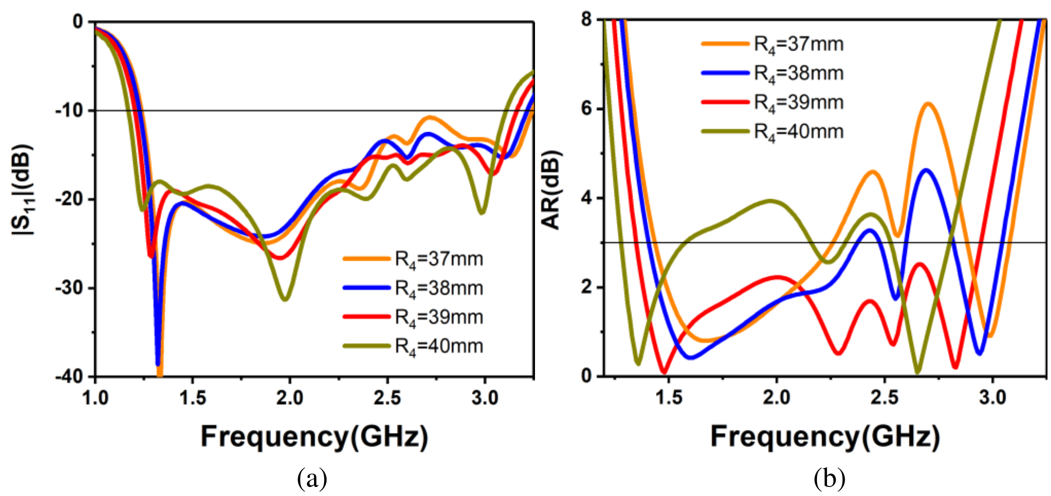


**Figure 5.** Parameter study of Ant.3: (a) $|S_{11}|$ and (b) AR varied with $R_4$.

be seen that the IBW of Ant.3 changes slightly with $R_4$. However when $R_4$ increases, the first and fourth CP resonant modes move to lower frequencies, and the second CP resonant mode (at about 2.3 GHz) becomes significant, but AR performance gets worse between the first and second CP resonant modes at the same time. As a compromise, we choose a medium value of 39 mm for a better CP performance.

Figure 6 depicts the effects of the rotation angle of the inverted L-shaped parasitic elements on

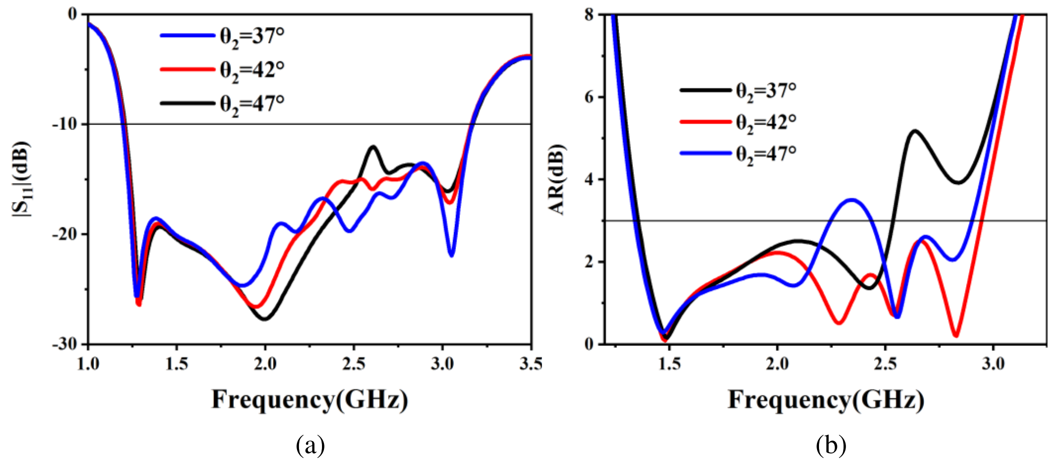


**Figure 6.** Parameter study of Ant.3: (a) $|S_{11}|$, (b) AR varied with $\theta_2$.

Ant.3. It can be seen from Figure 6(a) that rotation angle $\theta_2$ has little influence on impedance resonance characteristics of Ant.3. However when $\theta_2$ increases, AR performance gets better at high frequencies significantly. At the same time, the second CP mode moves to lower frequencies, and AR characteristics between the second and third CP mode get worse. Thus we choose 42° for $\theta_2$ as the optimized value.

## 3. RESULTS AND DISCUSSION

As seen in Figure 7, a prototype of the proposed antenna with optimized dimensions is fabricated and measured to test the operation performance. Four dielectric cylinders are added to fix the patch. The return loss of the proposed antenna is measured by an Agilent N5230A vector network analyzer. The AR, realized gain and radiation patterns are measured with multi-probe spherical Near Field System. Figure 8 shows the simulated and measured $|S_{11}|$, realized gain and AR along $+z$ axis for the proposed antenna. The antenna achieves an impedance bandwidth of 91.4% (1.20–3.22 GHz), and it can be seen that the measured and simulated $|S_{11}|$ are in good agreement. The measured 3-dB ARBW is 74.1% (1.37–2.98 GHz). Besides, the proposed antenna has stable realized gains range from 6.52 to 9.27 dBi over the whole operating band. The measured gains are a little smaller than the simulated results because of measurement and fabrication error. Figure 9 shows the simulated and measured normalized radiation patterns for the proposed antenna at 1.5, 2.3 and 2.8 GHz in $xoz$-plane and $yoz$-plane, respectively. It can be seen that the proposed antenna has unidirectional RHCP patterns along $+z$ direction. Low cross

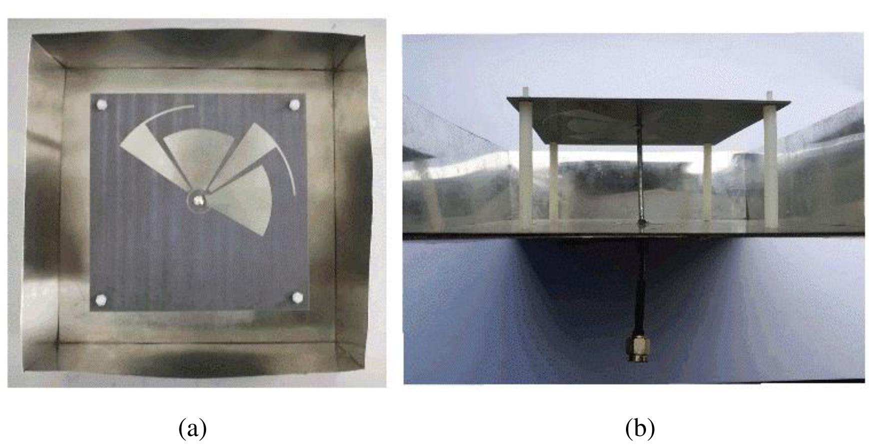


**Figure 7.** Photograph of the fabricated antenna: (a) top view, (b) side view.

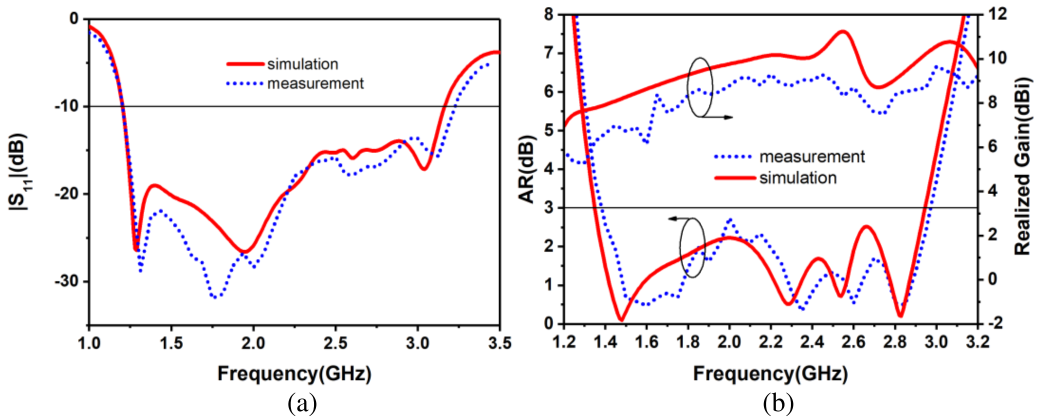


**Figure 8.** Simulated and measured results of proposed antenna: (a) $|S_{11}|$, (b) AR and realized gain.

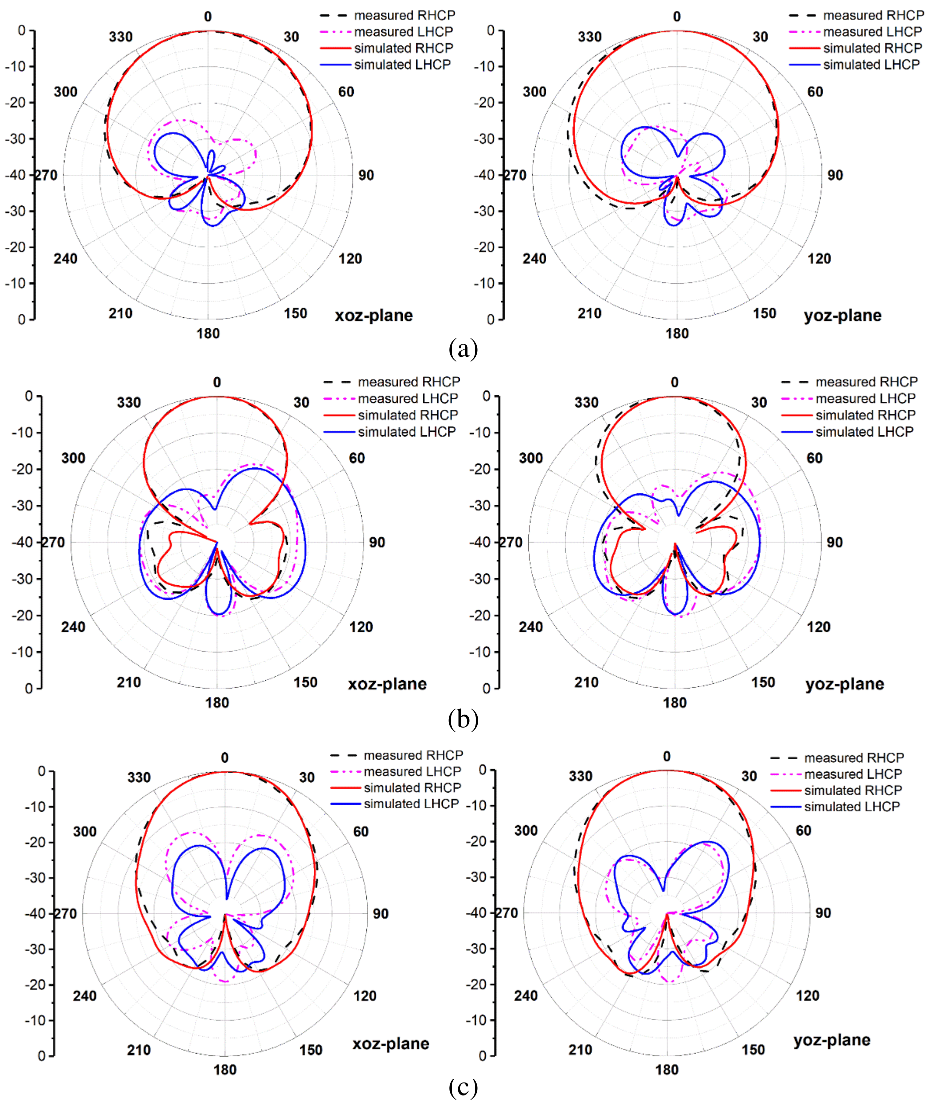


**Figure 9.** Simulated and measured normalized radiation pattern for proposed antenna at (a) 1.5 GHz, (b) 2.3 GHz, (c) 2.8 GHz.

**Table 1.** Performance comparison.

| Reference | Overall size ($\lambda_0^3$) | IBW | ARBW | Peak Gain | CP Mode |
|---|---|---|---|---|---|
| [1] | $0.742 \times 0.742 \times 0.265$ | 66.2% ($\lvert S_{11}\rvert \leq -10$ dB) | 47.8% | 7.1 dBi | 3 |
| [2] | $0.595 \times 0.595 \times 0.268$ | 37.1% (VSWR $\leq 2$) | 35.0% | $\sim 7.5$ dBi | 3 |
| [5] | $1.01 \times 1.01 \times 0.257$ | 57% ($\lvert S_{11}\rvert \leq -10$ dB) | 51.0% | 11 dBi | 3 |
| [6] | $\pi \times 0.514 \times 0.514 \times 0.257$ | 57.6% (VSWR $\leq 2$) | 39.2% | 10.7 dBi | 2 |
| [7] | $0.793 \times 0.793 \times 0.27$ | 68.9% ($\lvert S_{11}\rvert \leq -10$ dB) | 58.6% | 9.4 dBi | 2 |
| [9] | $1.1 \times 1.1 \times 0.28$ | 67.5% ($\lvert S_{11}\rvert \leq -10$ dB) | 53.4% | 10.62 dBi | 3 |
| Proposed | $1.01 \times 1.01 \times 0.29$ | 91.4% ($\lvert S_{11}\rvert \leq -10$ dB) | 74.1% | 9.27 dBi | 4 |

polarization is also generated over the whole operating band.

A comparison between the proposed antenna and previous works of the other CP antennas in literature is summarized in Table 1. Here $\lambda_0$ is the wavelength at the center frequency of the AR operating band. The peak gain of our work is smaller than that of the antennas in [5–7, 9], but our IBW and ARBW are much larger than theirs. The antenna in [2] has the smallest size, but its IBW and ARBW are comparatively narrow. The antennas in [5] and [6] have the lowest profile, but the ARBW is narrow. In conclusion, our work achieves a wider impedance and 3-dB AR bandwidth with extra CP resonate modes produced by the inverted L-shaped parasitic elements.

## 4. CONCLUSION

Inverted L-shaped parasitic elements with sequentially rotated angle has been introduced in circularly polarized crossed bowtie dipole for bandwidth enhancement in this letter. The proposed antenna excites four CP resonant modes and produces broadband unidirectional RHCP radiation with stable gains in the whole operating band. Some significant parameters are analyzed, and the proposed antenna is fabricated and measured. Results show that the proposed antenna achieves a wide impedance bandwidth of 91.4% (1.2–3.22 GHz) for $|S_{11}| < -10$ dB and a wide 3-dB ARBW of 74.1% (1.37–2.98 GHz). The excellent performance of its broadband CP characteristics and simple structure make it a candidate for wireless communication systems.

## REFERENCES

1. Xu, R., J. Y. Li, and K. Wei, "A broadband circularly polarized crossed-dipole antenna," *IEEE Transactions on Antennas & Propagation*, Vol. 64, 4509–4513, 2016.
2. Ding, X., Z. Zhao, Y. Yang, et al., "Broadband unidirectional printed antenna with quad-folded dipoles for circular polarization," *Microwave & Optical Technology Letters*, Vol. 57, 2871–2876, 2015.
3. Baik, J. W., K. J. Lee, W. S. Yoon, et al., "Circularly polarised printed crossed dipole antennas with broadband axial ratio," *Electronics Letters*, Vol. 44, 785–786, 2008.
4. Zhou, C. and S. W. Cheung, "High gain windmill-shaped CP antenna using high-order mode and ground-edge diffraction," *IEEE Antennas & Wireless Propagation Letters*, Vol. 99, 1–1, 2018.
5. Tran, H. H. and I. Park, "Wideband circularly polarized cavity-backed asymmetric crossed bowtie dipole antenna," *IEEE Antennas & Wireless Propagation Letters*, Vol. 15, 358–361, 2016.
6. Qu, S. W., C. H. Chan, and Q. Xue, "Wideband and high-gain composite cavity-backed crossed triangular bowtie dipoles for circularly polarized radiation," *IEEE Transactions on Antennas & Propagation*, Vol. 58, 3157–3164, 2010.
7. Tran, H. H., I. Park, and T. K. Nguyen, "Circularly polarized bandwidth-enhanced crossed dipole antenna with a simple single parasitic element," *IEEE Antennas & Wireless Propagation Letters*, Vol. 99, 1–1, 2017.

8. Baik, J. W., T. H. Lee, S. Pyo, et al., "Broadband circularly polarized crossed dipole with parasitic loop resonators and its arrays," *IEEE Transactions on Antennas & Propagation*, Vol. 59, 80–88, 2011.
9. Feng, G., L. Chen, X. Xue, et al., "Broadband circularly polarized crossed-dipole antenna with a single asymmetrical cross-loop," *IEEE Antennas & Wireless Propagation Letters*, Vol. 99, 1–1, 2017.
10. Wu, J., X. Ren, Z. Li, and Y.-Z. Yin, "Modified square slot antennas for broadband circular polarization," *Progress In Electromagnetics Research C*, Vol. 38, 1–14, 2013.
11. Chen, J. and J. Row, "A simple design for slotted patch antennas with broadband circular polarization," *Microwave & Optical Technology Letters*, Vol. 57, 1854–1857, 2015.